Highly potent human hematopoietic stem cells first emerge in the intraembryonic aorta-gonad-mesonephros region

Andrejs Ivanovs,[1] Stanislav Rybtsov,[1] Lindsey Welch,[3] Richard A. Anderson,[2] Marc L. Turner,[1,4] and Alexander Medvinsky[1]

[1]MRC Centre for Regenerative Medicine, University of Edinburgh, Edinburgh EH16 4UU, Scotland, UK
[2]MRC Centre for Reproductive Health, University of Edinburgh, Edinburgh EH16 4TJ, Scotland, UK
[3]Centre for Forensic Science, University of Strathclyde, Glasgow G1 1XW, Scotland, UK
[4]Scottish National Blood Transfusion Service, Edinburgh EH17 7QT, Scotland, UK

Hematopoietic stem cells (HSCs) emerge during embryogenesis and maintain hematopoiesis in the adult organism. Little is known about the embryonic development of human HSCs. We demonstrate that human HSCs emerge first in the aorta-gonad-mesonephros (AGM) region, specifically in the dorsal aorta, and only later appear in the yolk sac, liver, and placenta. AGM region cells transplanted into immunodeficient mice provide long-term high level multilineage hematopoietic repopulation. Human AGM region HSCs, although present in low numbers, exhibit a very high self-renewal potential. A single HSC derived from the AGM region generates at least 300 daughter HSCs in primary recipients, which disseminate throughout the entire recipient bone marrow and are retransplantable. These findings highlight the vast regenerative potential of the earliest human HSCs and set a new standard for in vitro generation of HSCs from pluripotent stem cells for the purpose of regenerative medicine.

CORRESPONDENCE
Alexander Medvinsky:
a.medvinsky@ed.ac.uk

Abbreviations used: AGM region, aorta-gonad-mesonephros region; CS, Carnegie stage; e.e., embryo equivalent; HSC, hematopoietic stem cell; NSG, NOD.Cg-*Prkdc*^{scid} *Il2rg*^{tm1Wjl}/Sz; STR, short tandem repeat; UCB, umbilical cord blood.

Hematopoietic stem cells (HSCs) are multipotent stem cells that emerge early during embryogenesis and maintain hematopoiesis throughout the entire lifespan of the organism (Dzierzak and Speck, 2008; Medvinsky et al., 2011). Although in various vertebrate species the first hematopoietic differentiation occurs in the yolk sac (Moore and Metcalf, 1970), a growing body of data suggests that the aorta-gonad-mesonephros (AGM) region plays a key role in the generation of definitive HSCs (Dieterlen-Lievre, 1975; Medvinsky et al., 1993; Müller et al., 1994; Medvinsky and Dzierzak, 1996; de Bruijn et al., 2002; Zovein et al., 2008; Boisset et al., 2010), possibly through hematopoietic transition of endothelial cells of the dorsal aorta, which has been most clearly shown in zebrafish (Bertrand et al., 2010; Kissa and Herbomel, 2010). The mouse AGM region is capable of autonomous initiation and expansion of HSCs (Medvinsky and Dzierzak, 1996; Cumano et al., 2001; Taoudi et al., 2008). The early umbilical cord and the placenta are also implicated in HSC development (de Bruijn et al., 2000; Gekas et al., 2005; Ottersbach and Dzierzak, 2005; Robin et al., 2009). In the mouse embryo, the first definitive HSCs are detected at approximately the same time in different tissues (Müller et al., 1994; de Bruijn et al., 2000; Kumaravelu et al., 2002; Gekas et al., 2005; Ottersbach and Dzierzak, 2005), thus their primary origin remains debatable (Medvinsky et al., 2011).

Qualitative and quantitative assessment of HSCs can only be performed functionally using in vivo limiting dilution long-term repopulation assays (Szilvassy et al., 1990). Although human HSCs have been extensively studied in fetal, neonatal, and adult sources by transplantation into immunodeficient mice (Larochelle et al., 1996; Conneally et al., 1997; Wang et al., 1997), at early embryonic stages HSCs were assayed only in the liver (Oberlin et al., 2010) and the placenta (Robin et al., 2009). To date, hematopoiesis in the AGM region and the yolk sac has been characterized only by immunohistological methods and in vitro assays (Tavian et al., 1996, 1999, 2001; Oberlin et al., 2002).

© 2011 Ivanovs et al. This article is distributed under the terms of an Attribution–Noncommercial–Share Alike–No Mirror Sites license for the first six months after the publication date (see http://www.rupress.org/terms). After six months it is available under a Creative Commons License (Attribution–Noncommercial–Share Alike 3.0 Unported license, as described at http://creativecommons.org/licenses/by-nc-sa/3.0/).

The Rockefeller University Press $30.00
J. Exp. Med. Vol. 208 No. 12 2417-2427
www.jem.org/cgi/doi/10.1084/jem.20111688

The Journal of Experimental Medicine

Downloaded from http://rupress.org/jem/article-pdf/208/12/2417/1911664/jem_20111688.pdf by guest on 04 December 2025

It is thought that HSCs mature in intraaortic cell clusters budding from the ventral wall of the dorsal aorta (Tavian et al., 1996, 1999; Jaffredo et al., 1998; Taoudi et al., 2008; Yokomizo and Dzierzak, 2010). The maturation of HSCs also occurs in deeper layers of the dorsal aorta (Rybtsov et al., 2011).

In this study, we describe spatiotemporal distribution of HSCs in the early human embryo and provide evidence that the AGM region is the first generator of highly potent HSCs in the human. Upon transplantation into immunodeficient mice, HSCs derived from the AGM region extensively propagate, migrate to different bones throughout the recipient, and provide progressively increasing long-term multilineage hematopoietic repopulation of the host animal with robust potential for retransplantation. Our study reveals that the first human HSCs possess an unprecedented self-renewal capacity. A better understanding of embryonic development of human HSCs may be instrumental for creating clinically relevant protocols for the production of HSCs from human embryonic and induced pluripotent stem cells (Kaufman, 2009).

RESULTS

Spatiotemporal distribution of HSCs in the early human embryo

AGM regions, yolk sacs, livers, umbilical cords, and placentas were obtained from human embryos between Carnegie stages (CSs) 12 and 17 (O'Rahilly and Müller, 1987). Cell suspensions prepared from these tissues were transplanted into irradiated NOD.Cg-*Prkdc*^{scid} *Il2rg*^{tm1Wjl}/Sz (NSG) mice (Shultz et al., 2005) within 3–4 h of termination of pregnancy. Cells from each individual tissue were split equally between two to four NSG recipient mice. In 27 independent experiments, HSCs were detected in 10 AGM regions and 3 yolk sacs by their capacity to provide human long-term (4–8 mo) multilineage hematopoietic repopulation and by their retransplantability into secondary recipients (Table I). In CS 14 and 15 human embryos, HSCs were detected exclusively in the AGM region (5 embryos). At CS 16 and 17, HSCs were found either solely in the AGM region (2 embryos) or both in the AGM region and the yolk sac (3 embryos). Thus, HSCs appear in the human AGM region at least 5 d earlier than in the yolk sac (Table I).

Out of 26 transplanted livers, none contained HSCs; however, two provided unilineage T cell engraftment (Table I and not depicted). In one case, exclusive T cell engraftment was also observed in a recipient of an AGM region (Table I and not depicted). In these three cases, human T cell contribution increased during the first 4–6 mo, and then decreased on a similar timescale (not depicted). Umbilical cords and placentas contained no HSCs at all stages tested (Table I).

Short tandem repeat (STR) analysis (Cotton et al., 2000) confirmed that the human cells detected in NSG recipient mice repopulated by AGM region, yolk sac, and liver cells originated from the donor embryo, with no evidence of contamination by maternal cells (Tables S1–S4).

The dorsal aorta is the source of HSC activity within the human AGM region

In the mouse embryo, definitive HSCs first appear in the dorsal aorta (de Bruijn et al., 2000; Taoudi and Medvinsky, 2007). We tested whether this is true for the human embryo. For these experiments, we used human embryos between CS 15 and 17. The human AGM region was subdissected into the dorsal aorta and the urogenital ridges, as previously described for the mouse AGM region (de Bruijn et al., 2000; Taoudi and Medvinsky, 2007). Cell suspensions prepared from these tissues were transplanted into irradiated NSG recipient mice. In 10 independent experiments performed, HSCs were detected in six dorsal aortas, but never in the urogenital ridges (see Materials and methods).

High-level hematopoietic repopulation by early embryonic HSCs

In NSG mice engrafted with human HSCs from the AGM region and the yolk sac, donor CD45$^+$ hematopoietic cells first became detectable in the peripheral blood of recipients 1.5–3 mo after transplantation, with donor cell levels reaching

Table I. The first HSCs in the human embryo emerge in the AGM region

Carnegie stage (days)	Embryonic tissues transplanted				
	AGM region	Yolk sac	Liver	Umbilical cord	Placentas
12 (26)	0/2	0/2	0/2	NA	1[c]/2
13 (28)	0/2	NA	0/1	NA	1[c]/2
14 (32)	1[a]/7	0/7	0/7	0/4	2[c]/7
15 (33)	4[a]/5	0/3	0/5	0/4	1[c]/2
16 (37)	2[a] + 1[b]/6	1[a]/4	0/6	0/6	1[c]/3
17 (41)	3[a]/5	2[a]/4	2[b]/5	0/3	1[c]/3
Total	10[a] + 1[b]/27	3[a]/20	2[b]/26	0/17	7[c]/19

Cell suspensions prepared from AGM regions, yolk sacs, livers, umbilical cords, and placenta obtained from CS 12–17 human embryos were individually transplanted into irradiated NSG mice. Data shown are the number of tissues that gave human hematopoietic repopulation compared to the total number of tissues transplanted. The numbers in parentheses indicate an approximate postovulatory gestational age in days accepted for each CS (O'Rahilly and Müller, 1987). NA, not assessed.

[a]Long-term embryonic multilineage repopulation.

[b]Long-term embryonic unilineage T cell repopulation.

[c]Transient maternal unilineage T cell repopulation.

Downloaded from http://rupress.org/jem/article-pdf/208/12/2417/1911664/jem_20111688.pdf by guest on 04 December 2025

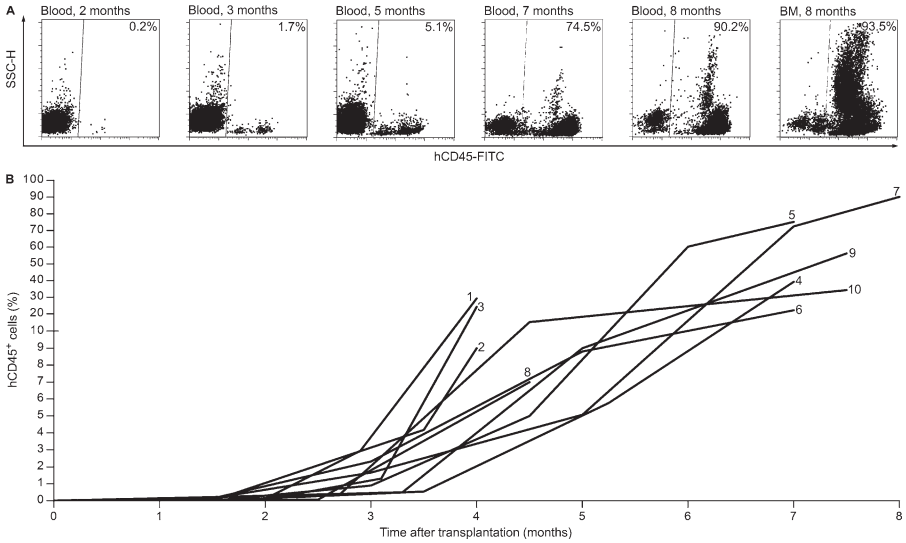

Figure 1. Human AGM region–derived HSCs provide progressive growth of hematopoietic contribution in NSG mice. (A) Representative flow cytometry plots show hematopoietic cells in the peripheral blood and BM of an NSG mouse transplanted with 0.33 e.e. of AGM region cells. In this case, the AGM region was obtained from a CS 16 embryo. The repopulation kinetics was monitored for 8 mo. hCD45, human CD45. (B) Human hematopoietic engraftment kinetics in the peripheral blood of 10 NSG recipient mice transplanted with human AGM region or yolk sac cells. The numbers at the end of the time series correspond to the recipient identification numbers in Table II.

repopulation in the peripheral blood by month 8 after transplantation (Notta et al., 2011).

~0.2% on average (range, 0.06–0.54%; $n = 13$) of total blood leukocytes. In all except one case, the percentage of human leukocytes in the peripheral blood progressively increased and reached up to 90% of total blood leukocytes by 8 mo after transplantation (Fig. 1 and Table II). By the end of the observation period (4–8 mo), on average ~40% (range, 7–90%; $n = 10$) of leukocytes in the recipient peripheral blood were of human origin (Fig. 1 and Table II). In the BM, the percentage of human $CD45^+$ cells was higher than in peripheral blood, reaching on average ~70% (range, 42–94%; $n = 7$) of total BM leukocytes (Table II). Previous studies have shown that transplantation of many human umbilical cord blood (UCB) or adult BM HSCs into immunodeficient mice results in blood chimerism that is <50% at 10 wk and frequently decreases after several months (Cashman et al., 1997; Ishikawa et al., 2005; Liu et al., 2010). However, recent experiments have shown that 10–20 UCB HSCs per one NSG recipient mouse are able to provide up to 40%

Multilineage differentiation potential of early embryonic HSCs

Human multilineage hematopoietic engraftment with AGM region and yolk sac cells was biased toward lymphopoiesis, dominated by B cells ($CD19^+$; Table III). Approximately one-third of human B cells in the recipient BM passed the pre–B cell stage, as indicated by the IgM expression on the cell surface. In the spleen, the proportion of human $CD19^+IgM^+$ cells was twice as high as in the BM, and in the peripheral blood almost all human B cells were IgM^+, replicating normal B cell development (Fig. 2 A). Human T cells ($CD3^+$) were also represented. Double-positive $CD4^+CD8^+$ cells prevailed in the thymus, and the peripheral blood contained mainly single-positive $CD4^+CD8^-$ and $CD8^+CD4^-$ T cells, which is indicative of normal intrathymic maturation of human T cells (Fig. 2 B and Table III). Almost all human T cells in the peripheral blood of recipient animals expressed αβ TCRs, as is observed in human peripheral blood. Only ~1% of T cells

Table II. High level hematopoietic repopulation by a single early embryonic HSC

Recipient no.	Tissues transplanted	Time after transplantation	Human $CD45^+$ cells in the recipient blood	Human $CD45^+$ cells in the recipient BM	Human $CD45^+$ cells in the recipient spleen
		mo	%	%	%
1	AGM region	4	29	42	4
2	AGM region	4	9	NA	NA
3	AGM region	4	24	45	31
4	AGM region	7	39	86	87
5	AGM region	7	73	93	93
6	AGM region	7	22	71	75
7	AGM region	8	90	94	96
8	Yolk sac	4.5	7	NA	NA
9	Yolk sac	7.5	56	NA	NA
10	Yolk sac	7.5	34	79	87

NSG mice transplanted with HSCs derived from the human AGM region or yolk sac were observed for 4–8 mo. At the end of each experiment, the percentage of human $CD45^+$ cells in the recipient peripheral blood, BM, and spleen was assessed by flow cytometry. NA, not assessed as the recipients died.

Downloaded from http://rupress.org/jem/article-pdf/208/12/2417/1911664/jem_20111688.pdf by guest on 04 December 2025

expressed γδ TCRs (Fig. 2 C). Additionally, human AGM region– and yolk sac–derived HSCs produced $CD94^+CD3^-$ NK cells and $CD94^+CD3^+$ NKT cells at low frequencies (Fig. 2 D and Table III).

The percentage of human $CD33^+$ myeloid cells in the recipient peripheral blood and spleen was ∼20–25 times lower than that of human lymphoid cells; however, the recipient BM contained on average 30% (range, 13–70; $n = 7$) human granulocytes ($CD33^+CD66b^+$) and monocytes ($CD33^+CD14^+$; Fig. 2 E and Table III). Megakaryocytic lineage was also readily detectable by appearance of human FSC-$H^{low}CD41a^+$ platelets in the recipient peripheral blood (Fig. 2 F). The recipient BM contained ∼8% human erythroid cells ($CD235a^+$), of which one third coexpressed CD45, indicating their immature state (Fig. 2 G).

Additionally, the BM of engrafted recipients plated into methylcellulose medium supplemented with human cytokines gave rise to human erythroid colonies (burst-forming units-erythroid [BFU-E]; Fig. 2 H and Table IV), myeloid colonies (colony-forming units-myeloid [CFU-Myeloid]; Table IV), and mixed erythromyeloid colonies (CFU-Mix; Fig. 2 I and Table IV). The human origin of hematopoietic colonies was confirmed by flow cytometry analysis (not depicted).

Early embryonic HSCs can be efficiently retransplanted

We tested whether HSCs derived from the human AGM region and yolk sac can be serially transplanted. In all eight experiments with the AGM region and two experiments with the yolk sac, transplantation of BM from primary recipients into secondary recipients resulted in sustainable human long-term multilineage hematopoietic engraftment (Fig. 3). In contrast, secondary BM transplantations from all three recipients exhibiting long-term unilineage T cell repopulation were unsuccessful. This indicates that HSCs colonize the human embryonic liver after CS 17. T cell–restricted repopulation may originate either from previously undescribed long-term persisting embryonic T cell progenitors or from human counterparts of mouse lymphopoiesis-biased γ and δ subtypes of long-term repopulating hematopoietic cells, which show no capacity for retransplantion (Dykstra et al., 2007).

Extensive amplification of early embryonic HSCs in primary recipients

Because one HSC can efficiently restore hematopoiesis in vivo (Osawa et al., 1996; Notta et al., 2011), the frequency of HSCs can be estimated using a limiting dilution assay (Szilvassy et al., 1990). In 9 out of 10 experiments transplanting human AGM region cells into two to four NSG mice, one recipient per experiment was found engrafted with human hematopoietic cells. Both recipients were repopulated in only one experiment (not depicted). To estimate HSC numbers, we used software for small numbers of replicates and nonlinear situations (Hu and Smyth, 2009). Our data fit the single-hit Poisson model ($\chi^2 = 0.108$; $P = 0.742$), demonstrating consistency between all 10 experiments performed with the AGM regions containing HSCs. The model calculations showed that one human AGM region contains ∼1.9 HSCs (95% CI, 1.0–3.3; Fig. 4 A). If all 23 CS 14–17 AGM regions are considered (including nonrepopulating ones), the frequency of HSCs is ∼0.8 per one human AGM region, which is close to the number of definitive HSCs in the mouse AGM region (Kumaravelu et al., 2002).

Statistically, human hematopoietic repopulation in each engrafted NSG mouse must have arisen mainly from one human HSC. The progressive growth in levels of repopulation with human hematopoietic cells (Fig. 1) may either be the result of gradual enhancement of productivity of this one HSC or, alternatively, the result of amplification of HSC numbers in recipients. To address this issue, the BM of engrafted primary recipients was harvested 4–8 mo after transplantation in five independent experiments. BM from an individual recipient was transferred into 6–15 secondary recipients. In these experiments, 41 out of 44 secondary recipients transplanted were found engrafted with human HSCs. Because each primary

Table III. Multilineage hematopoietic engraftment in primary recipient mice

Recipient no.	Blood				BM				Spleen				Thymus			
	B	T	NK	Myeloid	B	T	NK	Myeloid	B	T	NK	Myeloid	$CD4^-CD8^-$	$CD4^+CD8^+$	$CD4^+CD8^-$	$CD8^+CD4^-$
	% in gated human $CD45^+$ cells															
1	44	39	NA	11	48	19	NA	30	78	12	NA	9	NA	NA	NA	NA
2	67	23	3	4	NA	NA	NA	NA	NA	NA	NA	NA	NA	NA	NA	NA
3	19	65	5	11	16	42	1	38	29	56	1	15	1	68	25	6
4	77	5	4	12	51	0.1	0.2	45	87	1	1	9	2	84	10	4
5	75	19	2	4	62	1	0.3	37	90	7	0.7	2	3	80	13	4
6	56	25	9	9	61	19	1	20	82	4	3	14	2	85	9	4
7	17	36	31	18	20	4	1.5	74	41	39	11	11	NA	NA	NA	NA
8	59	22	NA	15	NA	NA	NA	NA	NA	NA	NA	NA	NA	NA	NA	NA
9	63	19	NA	14	NA	NA	NA	NA	NA	NA	NA	NA	NA	NA	NA	NA
10	26	60	9	6	42	12	2	43	46	41	7	7	2	69	22	7

Data shown are the percentage of B ($CD19^+$), T ($CD3^+$ or $CD4^+CD8^+$, $CD4^+CD8^-$, and $CD8^+CD4^-$), NK ($CD94^+CD3^-$), and myeloid cells ($CD33^+$ or $CD13^+$) in the human $CD45^+$ cell population in the peripheral blood, BM, spleen, and thymus of NSG mice transplanted with AGM region and yolk sac cells. The recipient identification numbers are the same as in Table II. NA, not assessed.

Downloaded from http://rupress.org/jem/article-pdf/208/12/2417/1911664/jem_20111688.pdf by guest on 04 December 2025

recipient was engrafted with approximately one human HSC, these results suggest that human HSCs propagated in primary recipients.

We considered an alternative possibility that the human AGM region contained some HSCs that remained dormant in primary recipients but could be activated upon secondary transplantations. To test this, we selected nonrepopulated primary recipients (Fig. 5 A, mice a and b) from five independent experiments in which at least one recipient was engrafted with AGM region cells (Fig. 5 A, mouse c). The entire BM from two coxal bones, two femurs, and two tibiae was collected from these nonrepopulated primary recipients and transferred into secondary recipients. None of secondary recipients showed human hematopoietic engraftment, confirming that the AGM region contained only one or two HSCs. Secondary transplantations of BM from nonengrafted recipients transplanted with yolk sac, liver, umbilical cord, and placental cells were also unsuccessful (two to five independent experiments were performed for each tissue).

To estimate the number of daughter HSCs generated in primary recipients by a single HSC derived from the AGM region, we performed two independent secondary transplantation experiments using the limiting dilution assay. The BM from successfully engrafted primary recipients was harvested from the sternum, humeri, ulnae, radii, coxal bones, femurs, and tibiae, and then pooled and transplanted in serial dilutions into secondary recipients. In experiment 1, the lowest dose transplanted per secondary recipient was 1/75 of total BM from primary recipient. All secondary recipients showed human long-term multilineage hematopoietic engraftment. In experiment 2, the transplanted dose was decreased further to 1/300 of total BM per recipient. Again, all secondary recipients showed human long-term multilineage hematopoietic repopulation (Fig. 4 B). However, in NSG mice transplanted with the lowest BM dose the level of human contribution, as determined in the peripheral blood 2 mo after transplantation, was <3%. Although we did not reach the limiting dose, we were close to the extinction of HSC activity. Human HSCs were also detected in spleens of primary recipients (Fig. 4 C). Thus, one HSC from the human AGM region is capable of generating at least 300 daughter HSCs upon transplantation. Previous studies have demonstrated a

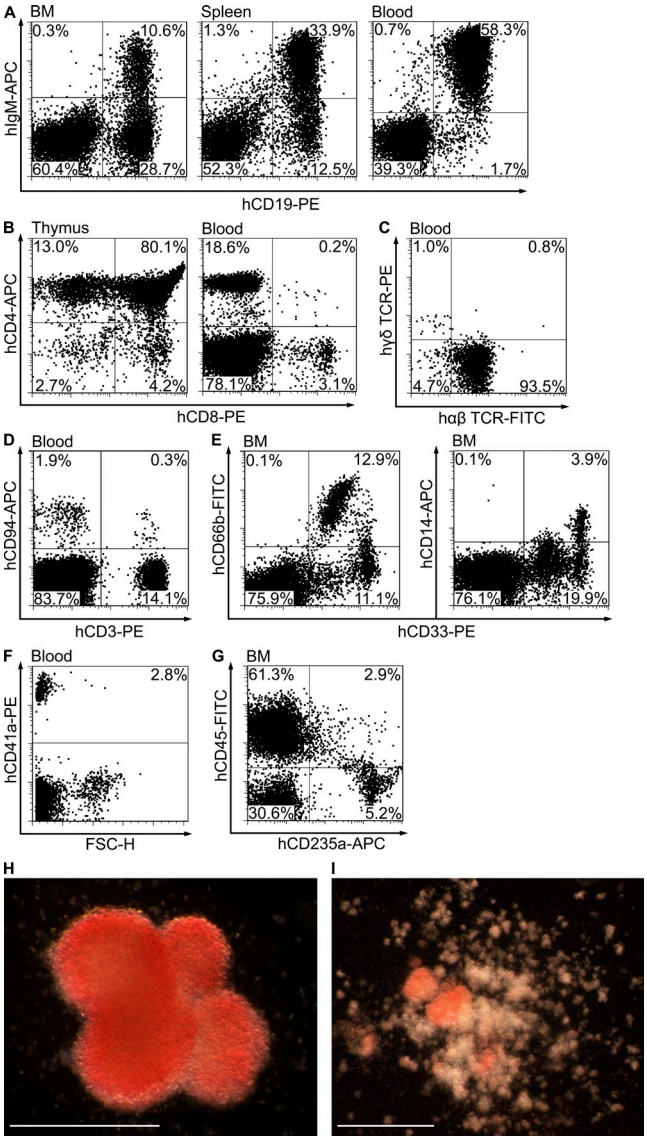

Figure 2. Human AGM region–derived HSCs provide long-term multilineage hematopoietic engraftment. Representative flow cytometry plots show human B cells (A), T cells (B and C), NK and NKT cells (D), granulocytes and monocytes (E), platelets (F), and erythroid cells (G) in the peripheral blood, BM, spleen, and/or thymus of an NSG mouse 7 mo after it was transplanted with 0.5 e.e. of AGM region cells. In this case, the AGM region was obtained from a CS 17 embryo. Note that the staining for CD4 and CD8 is shown in gated human $CD45^+$ cells, and for TCRs in gated human $CD3^+$ cells. Plating BM of the same recipient into methylcellulose medium supplemented with human cytokines resulted in the formation of human erythroid colonies (BFU-Es; H) and mixed erythromyeloid colonies (CFU-Mix; I). Bars, 0.5 mm.

Table IV. Human CFU-C frequency in the BM of primary recipient mice

Recipient no.	Human CFU-C no. per 10,000 input BM nucleated cells		
	BFU-E	CFU-Myeloid	CFU-Mix
1	2.3 ± 0.6	13.0 ± 3.8	2.5 ± 0.4
2	NA	NA	NA
3	8.7 ± 1.5	34.7 ± 11.2	1.7 ± 0.6
4	7.6 ± 1.4	26.1 ± 4.0	1.7 ± 0.2
5	5.0 ± 1.4	31.0 ± 1.4	0.5 ± 0.7
6	6.3 ± 0.1	16.3 ± 0.4	1.6 ± 0.3
7	6.5 ± 0.7	33.0 ± 4.2	1.5 ± 0.7
8	NA	NA	NA
9	NA	NA	NA
10	5.6 ± 0.6	15.4 ± 2.0	1.8 ± 0.3

Data shown are the number ± SD of human CFU-Cs per 10,000 input BM nucleated cells. The BM was obtained from NSG mice transplanted with AGM region and yolk sac cells. The recipient identification numbers are the same as in Table II. NA, not assessed, as the recipients died.

Downloaded from http://rupress.org/jem/article-pdf/208/12/2417/1911664/jem_20111688.pdf by guest on 04 December 2025

very limited self-renewal capacity by HSCs from the human UCB and adult BM (Guenechea et al., 2001; McKenzie et al., 2006; Liu et al., 2010). Although the microenvironment in immunodeficient mice is not optimal for the homeostatic expansion of human HSCs (Manz, 2007), human AGM region–derived HSCs extensively self-renew and amplify in these suboptimal conditions, suggesting that their expansion potential in physiological conditions is likely to be higher.

Extensive dissemination of daughter HSCs in primary recipients

The engraftment of one or two HSCs from the early human embryo results in considerable amplification of the HSC pool. We then tested if daughter HSCs stay at one site where the lodging of the parental HSC had occurred or if they migrate and disseminate throughout the recipient BM. We used two primary recipients repopulated with different AGM regions. We harvested BM from each recipient from the following six bones: two coxal bones, two femurs, and two tibiae (Fig. 5 A, mouse c). BM cell suspensions from each bone were transplanted separately into secondary recipients (Fig. 5 A, mice 1–6). In experiment 1, all secondary recipients showed human long-term multilineage hematopoietic engraftment (Fig. 5 B). Consistent with this, in experiment 2, all secondary recipients except one were repopulated with human hematopoietic cells. Thus, daughter HSCs generated by one or two human AGM region-derived HSCs disseminate broadly throughout the entire recipient BM.

Daughter HSCs are of the canonical phenotype

Using conventional FACS, it is not technically feasible to determine the immunophenotype of one or two HSCs present in one human AGM region. However, robust amplification of early embryonic HSCs in primary recipients allowed us to determine the immunophenotype of daughter HSCs. The BM harvested from the sternum, humeri, ulnae,

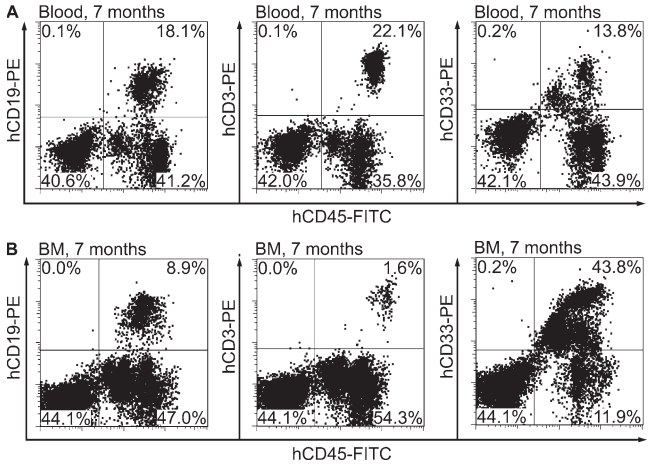

Figure 3. Human AGM region–derived HSCs provide long-term multilineage hematopoietic engraftment upon retransplantation into secondary recipients. Representative flow cytometry plots show human B ($CD19^+$), T ($CD3^+$), and myeloid cells ($CD33^+$) in the peripheral blood (A) and BM (B) of an NSG mouse transplanted with BM from a primary recipient engrafted with HSCs from a CS 15 AGM region. Secondary transplantation was performed 7 mo after primary transplantation. The analysis of secondary recipients was performed 7 mo later. Eight independent secondary transplantation experiments were performed.

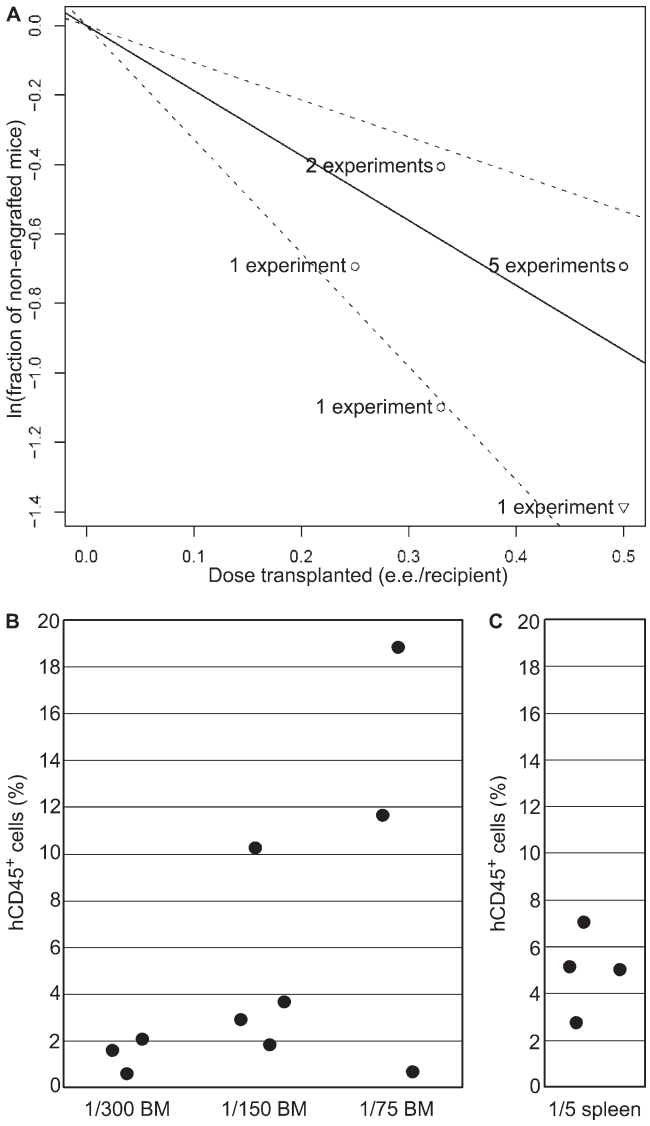

Figure 4. Extensive amplification of human AGM region–derived HSCs in primary recipients. (A) Results of 10 independent experiments in which HSCs were detected in AGM regions are plotted as the natural logarithm of the fraction of nonengrafted mice versus the dose of donor tissues (e.e. per recipient) transplanted in each experiment. The solid line shows the mean value. The dotted lines indicate 95% confidence interval. The data value with zero negative response (two out of two recipients were found engrafted with human HSCs) is represented by a down-pointing triangle. (B and C) 8 mo after transplantation, BM (B) and spleen (C) from a primary recipient repopulated with a single HSC from the AGM region of a CS 16 embryo were harvested and transplanted into secondary recipients (two independent experiments). Peripheral blood of secondary recipients was analyzed for human $CD45^+$ cell contribution 2 mo after transplantation. The ratios below the charts indicate the fraction of total BM or spleen transplanted per recipient.

Downloaded from http://rupress.org/jem/article-pdf/208/12/2417/1911664/jem_20111688.pdf by guest on 04 December 2025

radii, coxal bones, femurs, and tibiae of primary recipients engrafted with a single HSC from the human AGM region was sorted into four cell populations based on expression of human CD34 and CD38 antigens, and then transplanted into secondary recipients (Fig. 6 A). In two independent experiments, human HSCs were found exclusively within $CD34^+CD38^{-/lo}$ cell fraction (Fig. 6 B). Thus, HSCs derived from the early human embryo generate numerous HSCs of the canonical phenotype (Bhatia et al., 1997; McKenzie et al., 2006).

The human placenta develops HSCs later than the AGM region

In 19 independent experiments, we transplanted irradiated NSG mice with CS 12–17 placental cells and observed no long-term multilineage engraftment upon transplantation. Instead, in seven cases, placenta provided transient unilineage T cell repopulation of maternal origin (Table I, Table S5, and not depicted). The placenta contains maternal blood, and T cells from human blood can readily expand in immunodeficient mice (van Rijn et al., 2003). An older 15-wk-old placenta readily provided long-term multilineage hematopoietic repopulation of fetal origin in all three recipients (each received ~1/30 of total placental cells; Table S6 and not depicted). Thus, in contrast to the early CS 12–17 placenta, the midgestation human placenta does possess HSC activity. In the mouse embryo, definitive HSCs appear in the placenta concomitantly with the AGM region (Gekas et al., 2005; Ottersbach and Dzierzak, 2005).

DISCUSSION

Although the embryonic development of HSCs has been studied in various vertebrate species (Medvinsky et al., 2011), the generation of the first HSCs during human embryogenesis remains a largely unexplored topic. The present concept of the embryonic development of the human hematopoietic system is primarily based on morphological and in vitro studies (Tavian et al., 1996, 1999, 2001; Oberlin et al., 2002). By using functional in vivo long-term repopulation assays, we conducted systematic analysis of the spatiotemporal distribution of HSCs in the early human embryo. We have shown that the AGM region, more specifically the dorsal aorta, is the first generator of HSCs in the human. Interestingly, although in the mouse embryo definitive HSCs appear concomitantly in the AGM region, yolk sac, umbilical cord, and placenta (Müller et al., 1994; de Bruijn et al., 2000; Kumaravelu et al., 2002; Gekas et al., 2005; Ottersbach and Dzierzak, 2005), in the human embryo, the timing of HSC appearance in these sites is clearly

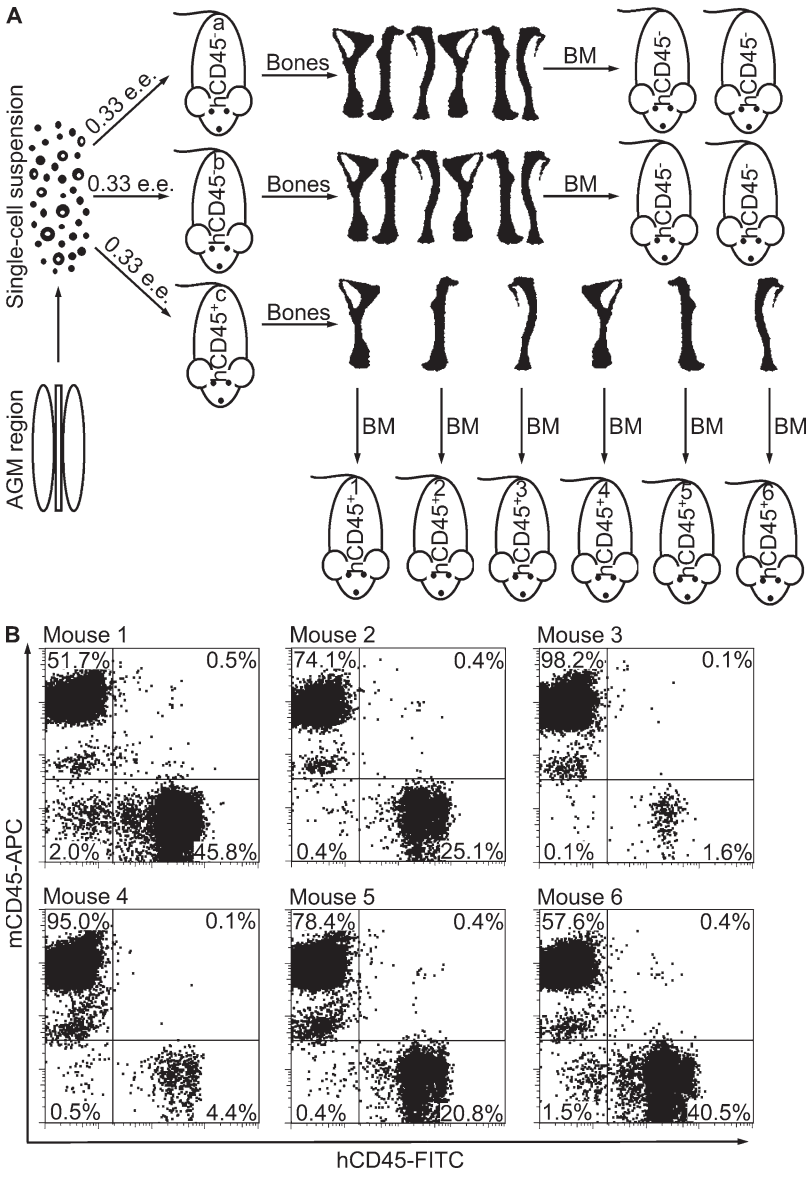

Figure 5. Extensive recipient BM colonization by daughter HSCs generated from a single AGM region–derived HSC. (A) AGM region cells obtained from a CS 15 embryo were transplanted into three NSG mice (0.33 e.e. per recipient). Only one of the three recipients showed human hematopoietic repopulation (mouse c). We confirmed by secondary transplantation that the other two recipients (mice a and b) contained no activatable HSCs. To test if the single human HSC that repopulated mouse c had generated daughter HSCs which could spread across the recipient BM, BM cells from two coxal bones, two femurs, and two tibiae were harvested and separately transplanted into six secondary recipients (mice 1–6). Secondary transplantations were performed 4 mo after the primary transplantation. (B) Representative flow cytometry plots show human hematopoietic repopulation in the peripheral blood of the six secondary recipients 3 mo later. Two independent experiments were performed. mCD45, mouse CD45.

Downloaded from http://rupress.org/jem/article-pdf/208/12/2417/1911664/jem_20111688.pdf by guest on 04 December 2025

resolved, possibly because of considerably longer development of the human embryo.

Our data indicate that early embryonic HSCs possess a considerably higher self-renewal capacity compared with UCB and adult BM HSCs (Guenechea et al., 2001; McKenzie et al., 2006; Liu et al., 2010). Upon transplantation into NSG mice, a single HSC from the human AGM region produces at least 300 daughter HSCs during a period of 8 mo; this unprecedented self-renewal capacity has not been previously described for human or for mouse AGM region–derived HSCs. It is likely because of this that the percentage of human leukocytes in the recipients' peripheral blood progressively increased, reaching up to 90% of total blood leukocytes. To achieve the same effect with UCB or adult BM, considerably higher numbers of HSCs need to be transplanted (Liu et al., 2010). More recent data suggest that ∼40% blood chimerism can be achieved 8 mo after transplantation of 10–20 UCB HSCs per one NSG mouse (Notta et al., 2011).

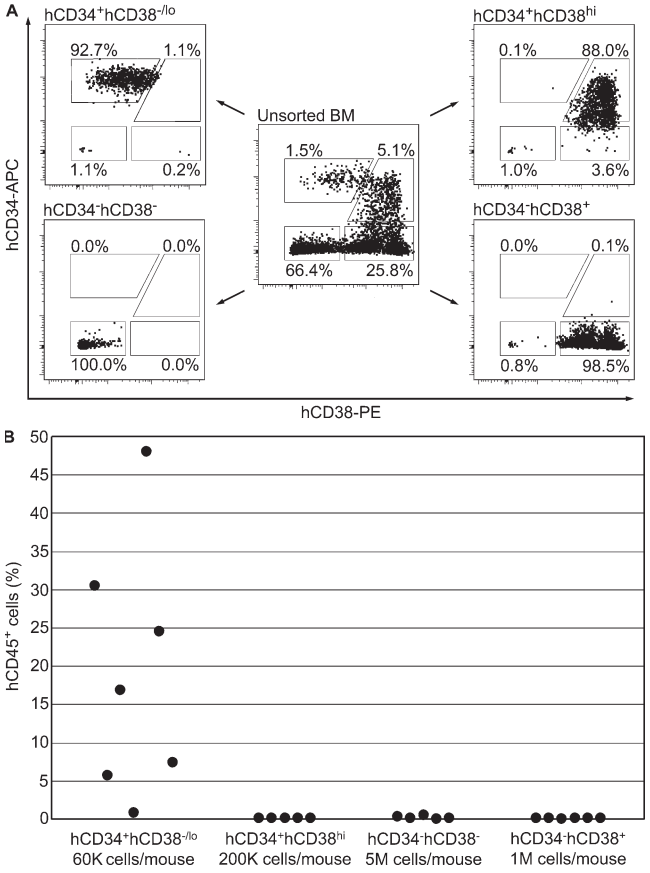

Figure 6. Daughter human AGM region–derived HSCs in primary recipients are CD34$^+$CD38$^{-/lo}$. (A) 7 mo after primary transplantation, BM of NSG mice repopulated with CS 16 and 17 AGM regions was sorted into four cell populations based on expression of human CD34 and CD38 antigens (two independent experiments). (B) Cells of each sorted population were injected into secondary recipients as indicated, and peripheral blood was analyzed 2 mo later. Two independent experiments were performed. K, multiple of thousand; M, multiple of million.

Using stochastic analyses, it has been shown that adult human HSCs replicate every 40 wk (Catlin et al., 2011). Our findings indicate that the extensive expansion of HSCs from the early human embryo occurs through replication every 3.5–4 wk or even more frequently, considering that HSCs also produce mature blood cells. This enormous regenerative capacity of early HSCs is consistent with them being founders of the adult hematopoietic system in the human.

We have shown that within the human AGM region HSCs emerge in the dorsal aorta. According to current views, it is possible that HSCs emerge in intraaortic cell clusters budding from the floor of the dorsal aorta (Jaffredo et al., 1998; Taoudi et al., 2008; Yokomizo and Dzierzak, 2010). In human, formation of such CD34$^+$CD45$^+$ cell clusters occurs between CS 12 and 16 (Tavian et al., 1996, 1999). Using limiting dilution analysis, we have shown that one human AGM region contains between one and three HSCs; however, the number of intraaortic cell clusters is much higher (Tavian et al., 1996, 1999), suggesting that not every cluster contains HSCs. Furthermore, although HSCs are still detected at CS 17, intraaortic cell clusters are reported to disappear by that stage (Tavian et al., 1996, 1999), indicating that the link between HSCs and hematopoietic cell clusters needs to be elucidated further. Notably, the maturation of definitive HSCs in the mouse embryo also occurs underneath the luminal layer of the dorsal aorta (Rybtsov et al., 2011).

As expected, HSC activity in the AGM region precedes that in the liver, which emerges there only after CS 17. Our data highlight the importance of in vivo long-term repopulation assays, as previous immunohistological and in vitro studies have suggested that HSCs appear in the human embryonic liver around CS 13 (Tavian et al., 1999). Recent transplantation experiments have shown that HSCs colonize the human embryonic liver around week 7–8 of development, which follows the stages we studied (Oberlin et al., 2010).

We demonstrate that in the human, in contrast to the mouse (Gekas et al., 2005; Ottersbach and Dzierzak, 2005), placenta acquires HSC activity long after the emergence of HSCs in the AGM region, indicating that in the human, placenta might be a secondary site for HSCs. Our data vary from a recent study's observation that the human placenta harbors HSCs from week 6 of development (as postmenstrual gestational age was employed, it is comparable with CS 12 or 13; Robin et al., 2009). In that study, NOD.CB17-*Prkdc*^{scid} (NOD/SCID) recipient mice, which are less receptive to human HSCs than NSG mice (McDermott et al., 2010), were used. The authors used a highly sensitive PCR analysis to detect repopulation with 6–8-wk-old placenta, identifying one human cell in 100,000 mouse cells. In the absence of flow cytometry analysis, a persistence of small numbers of some placenta-derived nonhematopoietic cells in recipients could not be excluded. However, the presence of multipotent HSCs in the placenta was convincingly shown by flow cytometry starting from week 9 of development (Robin et al., 2009).

Downloaded from http://rupress.org/jem/article-pdf/208/12/2417/1911664/jem_20111688.pdf by guest on 04 December 2025

In summary, we provide a systematic spatiotemporal picture of HSC emergence in the early human embryo and identify the AGM region as the primary source of HSCs with unprecedented self-renewal capacity. Future comparative studies of early human embryonic HSCs and their fetal, neonatal, and adult counterparts may shed light on the mechanisms of HSC self-renewal and aging.

MATERIALS AND METHODS

Human embryonic and fetal tissues. Human embryonic and fetal tissues were obtained immediately after elective termination of pregnancy. The procedure was performed using mifepristone and misoprostol. The study was approved by the Lothian Research Ethics Committee. Each patient gave informed consent in writing. The developmental stage of human embryos was determined according to the Carnegie staging system (O'Rahilly and Müller, 1987). The postmenstrual gestational age of human fetuses was determined using medical ultrasonography. Tissue dissection was performed in buffer 1 (PBS with Ca^{2+} and Mg^{2+} [Sigma-Aldrich] supplemented with 7% heat-inactivated FBS [PAA Laboratories], 100 IU/ml of penicillin [Invitrogen], and 100 μg/ml of streptomycin [Invitrogen]). The dissection procedure was similar to that previously described for the mouse embryo (Medvinsky et al., 2008). For the enzymatic treatment of the human AGM region, yolk sac, liver, and umbilical cord, 1 mg/ml of collagenase/dispase (Roche), and 0.12 mg/ml of DNase I (Roche) were added to buffer 1 and incubated at 37°C for 40 min. For the enzymatic treatment of placental tissue, two previously published protocols were employed (Bárcena et al., 2009; Robin et al., 2009). In the majority of experiments with the human placenta, we omitted the Ficoll-Paque density gradient separation step to minimize cell losses. By the end of enzymatic treatment, tissue digests were washed with buffer 2 which, compared with buffer 1, was made with Ca^{2+} and Mg^{2+}-free PBS. For preparation of placental cells, in contrast to other tissues, 2 mM of EDTA was added to this buffer. After the first wash with buffer 2, tissue digests were pipetted gently to prepare a single-cell suspension. Human AGM region, yolk sac, liver, and umbilical cord cells were washed an additional time with buffer 2. Placental cells were passed through a 40-μm nylon cell strainer (BD) and washed four more times. Finally, cells were resuspended in buffer 2 and kept on ice until transplantation. Throughout the manuscript "independent" refers to those experiments performed with different human embryos.

Long-term repopulation assays. NSG mice were used as recipients for human HSCs. Animals were housed and bred within the University of Edinburgh, Edinburgh, Scotland, UK. Experiments with animals were approved by the Animal Welfare Committee of the University of Edinburgh and were performed according to the provisions of the Animal (Scientific Procedures) Act 1986 under the project license granted by the Home Office. All researchers who performed experiments with the mice held personal licenses granted by the Home Office. Mice were kept under specific pathogen–free conditions. Acidified (pH 3.0) autoclaved water supplemented with 1.67 mg/ml of neomycin (Invitrogen) and γ-irradiated chow diet was provided ad libitum. Animals were exposed to 14-h light and 10-h dark cycle. Up to 6 h before transplantation with human cells, 6–8-wk-old female NSG mice received a sublethal total body irradiation dose of 3.5 Gy at a rate of 0.75 Gy/min from a ^{137}Cs source (GSR D1 γ-irradiator; Gamma-Service Medical). Animals were transplanted with cells intravenously via the tail vein. The number of transplanted embryonic cells was expressed in embryo equivalents (e.e.), defined as a unit of cells equivalent to the number present in one tissue. Starting from 6–8 wk after transplantation, NSG mice were bled by tail vein nicking every 1–2 mo, and human HSC contribution was assessed by flow cytometry analysis after labeling cells with anti–human CD45 antibody. At the end of each experiment (usually 4–8 mo after transplantation), all recipients (including those found nonengrafted after peripheral blood analysis) were killed by dislocation of the neck according to the Schedule 1 of the Animal (Scientific Procedures) Act 1986, and their BM was collected. BM cells were labeled with anti–human CD45 antibody, and flow cytometry analysis was performed to detect the presence of human hematopoietic cells. The peripheral blood, BM, spleen, and thymus of engrafted NSG mice were further analyzed by flow cytometry analysis. The BM and spleen from primary recipients were used in secondary transplantation experiments.

Recipient mouse tissues. To collect recipient mouse tissues, buffer 2 supplemented with 2 mM of EDTA was used. NSG mice transplanted with human AGM region, yolk sac, liver, umbilical cord, placental cells, or BM from primary recipients were bled by tail vein nicking, and erythrocytes were lysed using Pharm Lyse Buffer (BD) according to the manufacturer's instructions. To analyze hematopoietic tissues, the spleen, thymus, long bones, coxal bones, and sternum were obtained. Spleen and thymus were gently mashed in a small volume of the buffer through a 40-μm nylon cell strainer. The BM was flushed out from the bones, and a single-cell suspension was prepared by gentle pipetting. A cell fraction associated with endosteum was obtained from remaining bones after treatment with collagenase/dispase and DNase I at 37°C for 40 min and added to the flushed-out BM fraction. The cells were spun down, resuspended in buffer 2 and kept on ice until transplantation. To calculate the proportion of total BM transplanted into secondary recipients, we used previously reported data on the distribution of BM cells in different mouse bones (Boggs, 1984).

Human CFU-C assay. Human CFU-Cs in the BM of NSG recipient mice were detected by plating in triplicates 10,000–25,000 BM nucleated cells in the MethoCult H4034 Optimum Medium (StemCell Technologies) according to the manufacturer's recommendations. The BM from a nontransplanted NSG mouse was used as a negative control. Cells were incubated at 37°C in 5% CO_2 and ≥95% humidity for 14 d. Hematopoietic colonies were enumerated microscopically. Some individual colonies were subject to flow cytometry analysis after labeling hematopoietic cells with anti–human CD45 and CD235a and anti–mouse CD45 and Ter119 antibodies.

Antibodies, flow cytometry analysis, and FACS. The following mouse anti–human monoclonal antibodies (all from BD) were used for flow cytometry analysis and/or FACS: CD3-APC, PE, and PerCP (clones SK7 and SP34-2), CD4-APC and APC-Cy7 (clone RPA-T4), CD8-PE and PE-Cy7 (clone RPA-T8), CD11b-PE-Cy7 (clone ICRF44), CD13-APC (clone WM15), CD14-APC and APC-Cy7 (clones M5E2 and MφP9), CD19-PE (clone HIB19), CD33-PE (clone WM53), CD34-APC (clone 8G12), CD38-PE (clone HIT2), CD41a-FITC (HIP8), CD45-Biotin, FITC, and V450 (clone HI30), CD66b-FITC (clone G10F5), CD94-APC (clone HP-3D9), CD235a-APC (clone GA-R2), IgM-Biotin (clone G20-127), αβ TCR-FITC (clone WT31), γδ TCR-PE (clone 11F2). Appropriate isotype controls, streptavidin-APC, rat anti–mouse CD45-APC (clone 30-F11), and Ter119-PE and FITC were also purchased from BD. The Human FcR Blocking Reagent (Miltenyi Biotec) and anti–mouse CD16/32 purified monoclonal antibody (clone 93; eBioscience) were used to prevent unwanted binding of antibodies to Fc receptors. All of the aforementioned antibodies and reagents were used at final concentrations recommended by manufacturers or determined by in-house titration. Cell labeling and washes were performed in Ca^{2+} and Mg^{2+}-free PBS supplemented with 2% heat-inactivated FBS. For dead cell exclusion the buffer was supplemented with 1.5 μg/ml of 7-amino-actinomycin (eBioscience). A FACSCalibur (BD), LSRFortessa (BD), or CyAn ADP (Dako) instruments were used for flow cytometry analysis. FACS and postsort purity check were performed on a FACSAria II instrument (BD). Sorted cells were spun down, resuspended in buffer 2, and kept on ice until transplantation. Flow cytometry data were analyzed with FlowJo v7.6.1 software (Tree Star).

STR analysis. Genomic DNA was extracted from peripheral blood, spleen, and/or BM cells obtained from NSG mice repopulated with human hematopoietic cells and from embryonic or fetal donor tissues. For this, the QIAamp DNA Investigator Kit (QIAGEN) and a QIAcube robotic instrument (QIAGEN) were used. DNA quantification was performed with the Plexor HY System (Promega) and an Mx3500P real-time PCR machine (Stratagene).

Downloaded from http://rupress.org/jem/article-pdf/208/12/2417/1911664/jem_20111688.pdf by guest on 04 December 2025

DNA quantification values were determined using the Plexor Data Analysis Software (Promega). DNA samples and PCR positive and negative controls were amplified with the AmpFlSTR SGM Plus PCR Amplification Kit (Applied Biosystems). PCR products were detected on a 3130 Genetic Analyzer (Applied Biosystems). Handling of raw data and genotyping were performed with GeneMapper ID v3.2.1 software (Applied Biosystems). All the reagents and instruments listed above were used according to manufacturers' recommendations. DNA match probabilities were calculated based on allele frequencies in Scottish Caucasian population.

Limiting dilution analysis. Limiting dilution analysis was performed using ELDA software (Hu and Smyth, 2009) available at http://bioinf.wehi.edu.au/software/elda/.

Online supplemental material. Tables S1–S6 show STR analysis data confirming either embryonic or maternal origin of hematopoietic repopulation in recipients transplanted with human embryo or placenta-derived cells. Online supplemental material is available at http://www.jem.org/cgi/content/full/jem.20111688/DC1.

We thank the patients for donating tissues; research nurses A. Saunderson, J. Creiger, and I. Morton for patient recruitment; J. Verth, R. McInnes, C. Watt, C. Manson, and their staff for animal maintenance; S. Monard for cell sorting; P. Travers and K. Samuel for valuable advice; and S. Gordon-Keylock for useful comments on the manuscript.

Financial support for this study was provided by grants from the Leukaemia and Lymphoma Research (to A. Medvinsky), Medical Research Council (to A. Medvinsky and R.A. Anderson), Biotechnology and Biological Sciences Research Council (to A. Medvisnky), and Wellcome Trust (to A. Medvinsky). The Medical Research Council awarded A. Ivanovs with a PhD studentship.

Author contributions: A. Ivanovs performed the majority of transplantation experiments, interpreted experimental data, and wrote the manuscript; S. Rybtsov performed some transplantation experiments and interpreted experimental data; L. Welch performed STR analysis and interpreted its data; R.A. Anderson and M.L. Turner interpreted experimental data; and A. Medvisnky directed the study, interpreted experimental data, and wrote the manuscript.

The authors declare no competing financial interests.

Submitted: 11 August 2011
Accepted: 14 October 2011

REFERENCES

Bárcena, A., M. Kapidzic, M.O. Muench, M. Gormley, M.A. Scott, J.F. Weier, C. Ferlatte, and S.J. Fisher. 2009. The human placenta is a hematopoietic organ during the embryonic and fetal periods of development. *Dev. Biol.* 327:24–33. http://dx.doi.org/10.1016/j.ydbio.2008.11.017

Bertrand, J.Y., N.C. Chi, B. Santoso, S. Teng, D.Y. Stainier, and D. Traver. 2010. Haematopoietic stem cells derive directly from aortic endothelium during development. *Nature.* 464:108–111. http://dx.doi.org/10.1038/nature08738

Bhatia, M., J.C. Wang, U. Kapp, D. Bonnet, and J.E. Dick. 1997. Purification of primitive human hematopoietic cells capable of repopulating immune-deficient mice. *Proc. Natl. Acad. Sci. USA.* 94:5320–5325. http://dx.doi.org/10.1073/pnas.94.10.5320

Boggs, D.R. 1984. The total marrow mass of the mouse: a simplified method of measurement. *Am. J. Hematol.* 16:277–286. http://dx.doi.org/10.1002/ajh.2830160309

Boisset, J.C., W. van Cappellen, C. Andrieu-Soler, N. Galjart, E. Dzierzak, and C. Robin. 2010. In vivo imaging of haematopoietic cells emerging from the mouse aortic endothelium. *Nature.* 464:116–120. http://dx.doi.org/10.1038/nature08764

Cashman, J.D., T. Lapidot, J.C. Wang, M. Doedens, L.D. Shultz, P. Lansdorp, J.E. Dick, and C.J. Eaves. 1997. Kinetic evidence of the regeneration of multilineage hematopoiesis from primitive cells in normal human bone marrow transplanted into immunodeficient mice. *Blood.* 89:4307–4316.

Catlin, S.N., L. Busque, R.E. Gale, P. Guttorp, and J.L. Abkowitz. 2011. The replication rate of human hematopoietic stem cells in vivo. *Blood.* 117:4460–4466. http://dx.doi.org/10.1182/blood-2010-08-303537

Conneally, E., J. Cashman, A. Petzer, and C. Eaves. 1997. Expansion in vitro of transplantable human cord blood stem cells demonstrated using a quantitative assay of their lympho-myeloid repopulating activity in nonobese diabetic-scid/scid mice. *Proc. Natl. Acad. Sci. USA.* 94:9836–9841. http://dx.doi.org/10.1073/pnas.94.18.9836

Cotton, E.A., R.F. Allsop, J.L. Guest, R.R. Frazier, P. Koumi, I.P. Callow, A. Seager, and R.L. Sparkes. 2000. Validation of the AMPFlSTR SGM plus system for use in forensic casework. *Forensic Sci. Int.* 112:151–161. http://dx.doi.org/10.1016/S0379-0738(00)00182-1

Cumano, A., J.C. Ferraz, M. Klaine, J.P. Di Santo, and I. Godin. 2001. Intraembryonic, but not yolk sac hematopoietic precursors, isolated before circulation, provide long-term multilineage reconstitution. *Immunity.* 15:477–485. http://dx.doi.org/10.1016/S1074-7613(01)00190-X

de Bruijn, M.F., N.A. Speck, M.C. Peeters, and E. Dzierzak. 2000. Definitive hematopoietic stem cells first develop within the major arterial regions of the mouse embryo. *EMBO J.* 19:2465–2474. http://dx.doi.org/10.1093/emboj/19.11.2465

de Bruijn, M.F., X. Ma, C. Robin, K. Ottersbach, M.J. Sanchez, and E. Dzierzak. 2002. Hematopoietic stem cells localize to the endothelial cell layer in the midgestation mouse aorta. *Immunity.* 16:673–683. http://dx.doi.org/10.1016/S1074-7613(02)00313-8

Dieterlen-Lievre, F. 1975. On the origin of haemopoietic stem cells in the avian embryo: an experimental approach. *J. Embryol. Exp. Morphol.* 33: 607–619.

Dykstra, B., D. Kent, M. Bowie, L. McCaffrey, M. Hamilton, K. Lyons, S.J. Lee, R. Brinkman, and C. Eaves. 2007. Long-term propagation of distinct hematopoietic differentiation programs in vivo. *Cell Stem Cell.* 1:218–229. http://dx.doi.org/10.1016/j.stem.2007.05.015

Dzierzak, E., and N.A. Speck. 2008. Of lineage and legacy: the development of mammalian hematopoietic stem cells. *Nat. Immunol.* 9:129–136. http://dx.doi.org/10.1038/ni1560

Gekas, C., F. Dieterlen-Lièvre, S.H. Orkin, and H.K. Mikkola. 2005. The placenta is a niche for hematopoietic stem cells. *Dev. Cell.* 8:365–375. http://dx.doi.org/10.1016/j.devcel.2004.12.016

Guenechea, G., O.I. Gan, C. Dorrell, and J.E. Dick. 2001. Distinct classes of human stem cells that differ in proliferative and self-renewal potential. *Nat. Immunol.* 2:75–82. http://dx.doi.org/10.1038/83199

Hu, Y., and G.K. Smyth. 2009. ELDA: extreme limiting dilution analysis for comparing depleted and enriched populations in stem cell and other assays. *J. Immunol. Methods.* 347:70–78. http://dx.doi.org/10.1016/j.jim.2009.06.008

Ishikawa, F., M. Yasukawa, B. Lyons, S. Yoshida, T. Miyamoto, G. Yoshimoto, T. Watanabe, K. Akashi, L.D. Shultz, and M. Harada. 2005. Development of functional human blood and immune systems in NOD/SCID/IL2 receptor γ chain$^{(null)}$ mice. *Blood.* 106:1565–1573. http://dx.doi.org/10.1182/blood-2005-02-0516

Jaffredo, T., R. Gautier, A. Eichmann, and F. Dieterlen-Lièvre. 1998. Intraaortic hemopoietic cells are derived from endothelial cells during ontogeny. *Development.* 125:4575–4583.

Kaufman, D.S. 2009. Toward clinical therapies using hematopoietic cells derived from human pluripotent stem cells. *Blood.* 114:3513–3523. http://dx.doi.org/10.1182/blood-2009-03-191304

Kissa, K., and P. Herbomel. 2010. Blood stem cells emerge from aortic endothelium by a novel type of cell transition. *Nature.* 464:112–115. http://dx.doi.org/10.1038/nature08761

Kumaravelu, P., L. Hook, A.M. Morrison, J. Ure, S. Zhao, S. Zuyev, J. Ansell, and A. Medvinsky. 2002. Quantitative developmental anatomy of definitive haematopoietic stem cells/long-term repopulating units (HSC/RUs): role of the aorta-gonad-mesonephros (AGM) region and the yolk sac in colonisation of the mouse embryonic liver. *Development.* 129:4891–4899.

Larochelle, A., J. Vormoor, H. Hanenberg, J.C. Wang, M. Bhatia, T. Lapidot, T. Moritz, B. Murdoch, X.L. Xiao, I. Kato, et al. 1996. Identification of primitive human hematopoietic cells capable of repopulating NOD/SCID mouse bone marrow: implications for gene therapy. *Nat. Med.* 2:1329–1337. http://dx.doi.org/10.1038/nm1296-1329

Downloaded from http://rupress.org/jem/article-pdf/208/12/2417/1911664/jem_20111688.pdf by guest on 04 December 2025

Liu, C., B.J. Chen, D. Deoliveira, G.D. Sempowski, N.J. Chao, and R.W. Storms. 2010. Progenitor cell dose determines the pace and completeness of engraftment in a xenograft model for cord blood transplantation. *Blood*. 116:5518–5527. http://dx.doi.org/10.1182/blood-2009-12-260810

Manz, M.G. 2007. Human-hemato-lymphoid-system mice: opportunities and challenges. *Immunity*. 26:537–541. http://dx.doi.org/10.1016/j.immuni.2007.05.001

McDermott, S.P., K. Eppert, E.R. Lechman, M. Doedens, and J.E. Dick. 2010. Comparison of human cord blood engraftment between immunocompromised mouse strains. *Blood*. 116:193–200. http://dx.doi.org/10.1182/blood-2010-02-271841

McKenzie, J.L., O.I. Gan, M. Doedens, J.C. Wang, and J.E. Dick. 2006. Individual stem cells with highly variable proliferation and self-renewal properties comprise the human hematopoietic stem cell compartment. *Nat. Immunol*. 7:1225–1233. http://dx.doi.org/10.1038/ni1393

Medvinsky, A., and E. Dzierzak. 1996. Definitive hematopoiesis is autonomously initiated by the AGM region. *Cell*. 86:897–906. http://dx.doi.org/10.1016/S0092-8674(00)80165-8

Medvinsky, A.L., N.L. Samoylina, A.M. Müller, and E.A. Dzierzak. 1993. An early pre-liver intraembryonic source of CFU-S in the developing mouse. *Nature*. 364:64–67. http://dx.doi.org/10.1038/364064a0

Medvinsky, A., S. Taoudi, S. Mendes, and E. Dzierzak. 2008. Analysis and manipulation of hematopoietic progenitor and stem cells from murine embryonic tissues. *Curr. Protoc. Stem Cell Biol*. Chapter 2:2A: 6.

Medvinsky, A., S. Rybtsov, and S. Taoudi. 2011. Embryonic origin of the adult hematopoietic system: advances and questions. *Development*. 138:1017–1031. http://dx.doi.org/10.1242/dev.040998

Moore, M.A., and D. Metcalf. 1970. Ontogeny of the haemopoietic system: yolk sac origin of in vivo and in vitro colony forming cells in the developing mouse embryo. *Br. J. Haematol*. 18:279–296. http://dx.doi.org/10.1111/j.1365-2141.1970.tb01443.x

Müller, A.M., A. Medvinsky, J. Strouboulis, F. Grosveld, and E. Dzierzak. 1994. Development of hematopoietic stem cell activity in the mouse embryo. *Immunity*. 1:291–301. http://dx.doi.org/10.1016/1074-7613(94)90081-7

Notta, F., S. Doulatov, E. Laurenti, A. Poeppl, I. Jurisica, and J.E. Dick. 2011. Isolation of single human hematopoietic stem cells capable of long-term multilineage engraftment. *Science*. 333:218–221. http://dx.doi.org/10.1126/science.1201219

O'Rahilly, R., and F. Müller. 1987. Developmental stages in human embryos. Carnegie Institution of Washington, Washington. 306 pp.

Oberlin, E., M. Tavian, I. Blazsek, and B. Péault. 2002. Blood-forming potential of vascular endothelium in the human embryo. *Development*. 129:4147–4157.

Oberlin, E., M. Fleury, D. Clay, L. Petit-Cocault, J.J. Candelier, B. Mennesson, T. Jaffredo, and M. Souyri. 2010. VE-cadherin expression allows identification of a new class of hematopoietic stem cells within human embryonic liver. *Blood*. 116:4444–4455. http://dx.doi.org/10.1182/blood-2010-03-272625

Osawa, M., K. Hanada, H. Hamada, and H. Nakauchi. 1996. Long-term l ymphohematopoietic reconstitution by a single CD34-low/negative hematopoietic stem cell. *Science*. 273:242–245. http://dx.doi.org/10.1126/science.273.5272.242

Ottersbach, K., and E. Dzierzak. 2005. The murine placenta contains hematopoietic stem cells within the vascular labyrinth region. *Dev. Cell*. 8:377–387. http://dx.doi.org/10.1016/j.devcel.2005.02.001

Robin, C., K. Bollerot, S. Mendes, E. Haak, M. Crisan, F. Cerisoli, I. Lauw, P. Kaimakis, R. Jorna, M. Vermeulen, et al. 2009. Human placenta is a potent hematopoietic niche containing hematopoietic stem and progenitor cells throughout development. *Cell Stem Cell*. 5:385–395. http://dx.doi.org/10.1016/j.stem.2009.08.020

Rybtsov, S., M. Sobiesiak, S. Taoudi, C. Souilhol, J. Senserrich, A. Liakhovitskaia, A. Ivanovs, J. Frampton, S. Zhao, and A. Medvinsky. 2011. Hierarchical organization and early hematopoietic specification of the developing HSC lineage in the AGM region. *J. Exp. Med*. 208:1305–1315. http://dx.doi.org/10.1084/jem.20102419

Shultz, L.D., B.L. Lyons, L.M. Burzenski, B. Gott, X. Chen, S. Chaleff, M. Kotb, S.D. Gillies, M. King, J. Mangada, et al. 2005. Human lymphoid and myeloid cell development in NOD/LtSz-scid IL2R γ^{null} mice engrafted with mobilized human hemopoietic stem cells. *J. Immunol*. 174:6477–6489.

Szilvassy, S.J., R.K. Humphries, P.M. Lansdorp, A.C. Eaves, and C.J. Eaves. 1990. Quantitative assay for totipotent reconstituting hematopoietic stem cells by a competitive repopulation strategy. *Proc. Natl. Acad. Sci. USA*. 87:8736–8740. http://dx.doi.org/10.1073/pnas.87.22.8736

Taoudi, S., and A. Medvinsky. 2007. Functional identification of the hematopoietic stem cell niche in the ventral domain of the embryonic dorsal aorta. *Proc. Natl. Acad. Sci. USA*. 104:9399–9403. http://dx.doi.org/10.1073/pnas.0700984104

Taoudi, S., C. Gonneau, K. Moore, J.M. Sheridan, C.C. Blackburn, E. Taylor, and A. Medvinsky. 2008. Extensive hematopoietic stem cell generation in the AGM region via maturation of VE-cadherin$^+$CD45$^+$ pre-definitive HSCs. *Cell Stem Cell*. 3:99–108. http://dx.doi.org/10.1016/j.stem.2008.06.004

Tavian, M., L. Coulombel, D. Luton, H.S. Clemente, F. Dieterlen-Lièvre, and B. Péault. 1996. Aorta-associated CD34$^+$ hematopoietic cells in the early human embryo. *Blood*. 87:67–72.

Tavian, M., M.F. Hallais, and B. Péault. 1999. Emergence of intraembryonic hematopoietic precursors in the pre-liver human embryo. *Development*. 126:793–803.

Tavian, M., C. Robin, L. Coulombel, and B. Péault. 2001. The human embryo, but not its yolk sac, generates lympho-myeloid stem cells: mapping multipotent hematopoietic cell fate in intraembryonic mesoderm. *Immunity*. 15:487–495. http://dx.doi.org/10.1016/S1074-7613(01)00193-5

van Rijn, R.S., E.R. Simonetti, A. Hagenbeek, M.C. Hogenes, R.A. de Weger, M.R. Canninga-van Dijk, K. Weijer, H. Spits, G. Storm, L. van Bloois, et al. 2003. A new xenograft model for graft-versus-host disease by intravenous transfer of human peripheral blood mononuclear cells in RAG2$^{-/-}$ gammac$^{-/-}$ double-mutant mice. *Blood*. 102:2522–2531. http://dx.doi.org/10.1182/blood-2002-10-3241

Wang, J.C., M. Doedens, and J.E. Dick. 1997. Primitive human hematopoietic cells are enriched in cord blood compared with adult bone marrow or mobilized peripheral blood as measured by the quantitative in vivo SCID-repopulating cell assay. *Blood*. 89:3919–3924.

Yokomizo, T., and E. Dzierzak. 2010. Three-dimensional cartography of hematopoietic clusters in the vasculature of whole mouse embryos. *Development*. 137:3651–3661. http://dx.doi.org/10.1242/dev.051094

Zovein, A.C., J.J. Hofmann, M. Lynch, W.J. French, K.A. Turlo, Y. Yang, M.S. Becker, L. Zanetta, E. Dejana, J.C. Gasson, et al. 2008. Fate tracing reveals the endothelial origin of hematopoietic stem cells. *Cell Stem Cell*. 3:625–636. http://dx.doi.org/10.1016/j.stem.2008.09.018

Downloaded from http://rupress.org/jem/article-pdf/208/12/2417/1911664/jem_20111688.pdf by guest on 04 December 2025